NATURAL FREQUENCIES OF CANTILEVERED TRIANGULAR TAPERED PLATES

by

DALLAS R. KOERNER

B. S., Kansas State University, 1963

A MASTER'S THESIS

submitted in partial fulfillment of the

requirements for the degree

MASTER OF SCIENCE

Department of Civil Engineering

KANSAS STATE UNIVERSITY

Manhattan, Kansas

1966

Approved by:

Major Professor

LD
2668
T4
1966
K98
C.2
Document

TABLE OF CONTENTS

FIGURES AND TABLES

SUMMARY

This study is concerned with the vibrations problem connected with variable-thickness plate structures. The method of analysis employed in this study was first introduced by John C. Houbolt (1) in his doctoral thesis. This method utilizes finite-difference equations in conjunction with the principle of minimum potential energy. High-speed computing equipment is a necessity if this method is to be used to its full potential.

The applications consisted of computing the natural frequencies for a series of cantilevered triangular variable-thickness plates. The nodal patterns were computed for the purpose of comparison with present and future experimental results. Computed frequencies and nodal patterns for the first five modes of vibration are shown. Experimental results from other investigations are compared with computed results whenever possible. On the basis of these comparisons, it is concluded that the method is accurate in approximating natural frequencies and nodal patterns for the type of plates analyzed and further applications are suggested.

Appendix C is devoted to computing procedures used in conjunction with the high-speed computing equipment. Actual computer programs written specifically for this paper are presented and discussed.

Appendix B contains computed nodal patterns for which experimental confirmation is not presently available.

INTRODUCTION

At the present time there is very little information available to insure proper usage of tapered sheet material being produced for the aircraft and missile industry. Within the last decade tapered sheet material has become available in great quantity and therefore characteristics of tapered plates are in demand. This study provides information concerning the characteristics of vibrating tapered triangular plates.

Although literature on the flexure of variable-thickness plate structures has been in existence since about 1930, it has not been until the recent missile age that work has been done on the vibrations problem connected with these structures. Along with the space and missile age has come the high-speed computing equipment which now makes it possible to solve these complex problems. John C. Houbolt (1), in his doctoral thesis, proposed an approximate technique well adapted for use with high-speed computers which is directly applicable to calculating plate bending. In principle, the technique consists of approximating partial differential equations by finite-difference equations in conjunction with the principle of minimum potential energy and may be applied to plates of any planform or taper ratio.

William Walton (2) reviewed Houbolt's method and extended it to the vibrations problem but restricted his work to uniform-thickness plates. This paper is concerned with the application of the same basic method but to variable-thickness plates.

Applications consist of calculations of the natural frequencies and nodal patterns of several triangular tapered plates.

As a basis for evaluating the method, computed results are compared with experimental results from other investigations whenever possible. As a means of checking computer programs, computed values for the first frequencies of a series of square plates are compared with values found by another approximate technique (3).

The computer programs used in this study are presented and discussed in Appendix C.

REVIEW OF LITERATURE

In 1951, M. V. Barton (4) investigated the natural vibrations problem connected with rectangular and skew cantilevered plates. In his work Barton used a Ritz approximation technique to find values for the natural frequencies and their corresponding nodal patterns. This work was restricted to homogeneous uniform thickness elastic plates corresponding to ordinary thin plate theory.

In 1952, J. W. Dalley and E. A. Ripperger (5) experimented with plates of the same type. In their investigations resonant frequencies were obtained by observing the forced oscillations of a plate when a pulsating air stream was directed normal to it. Electronic devices were used to record these resonant frequencies.

Another experimental study of the natural vibrations of thin plates was conducted in 1953 by P. N. Gustafson, W. F. Stokey, and C. F. Zorowski (6). Their investigations considered triangular shaped plates. By use of a simple electromagnetic driving mechanism and other electronic devices they were able to obtain values for the first six natural frequencies as well as the corresponding nodal patterns.

In his doctoral thesis in 1957, John C. Houbolt (1) introduced a method of calculating plate bending. This method utilizes finite-difference approximations in conjunction with a variational principle. However, Houbolt restricted his work with this method to the calculation of moments and deflections for uniform-

thickness plate structures. William Walton (2) in 1958 applied this method to the vibrations problem of plates. He used Houbolt's method to compute approximate values for the first six natural frequencies and their corresponding nodal patterns for a series of cantilevered plates. Although he extended Houbolt's method in general terms, Walton limited his work to the uniform-thickness problem.

Fred Appl and N. R. Byers (3), in 1964, used a bounding technique to find both upper and lower bounds for the fundamental frequency of several variable-thickness rectangular plates. This bounding technique was found to be very accurate.

REVIEW OF HOUBOLT'S METHOD OF ANALYSIS

Let W(x,y) describe local deflections of a plate at equilibrium under a load p(x,y) acting normal to the coordinate plane of the plate. Then following ordinary thin plate theory, the total potential energy, denoted as U, is given by the equation

$$U = \iint \left\{ \frac{D(x,y)}{2} \left[\left(\frac{\partial^2 W(x,y)}{\partial x^2} + \frac{\partial^2 W(x,y)}{\partial y^2} \right)^2 - 2(1-\upsilon) \left(\frac{\partial^2 W(x,y)}{\partial x^2} \right) \left(\frac{\partial^2 W(x,y)}{\partial y^2} \right) - \left(\frac{\partial^2 W(x,y)}{\partial x \, \partial y} \right)^2 \right] - p(x,y)W(x,y) \right\} dx \, dy \tag{1}$$

which can be written in the form

$$U = \iint_A B(x,y)dx \, dy + \iint_A C(x,y)dx \, dy \tag{1A}$$

in which

$$B(x,y) = \frac{D(x,y)}{2} \left[\left(\frac{\partial^2 W(x,y)}{\partial x^2} \right)^2 + \left(\frac{\partial^2 W(x,y)}{\partial y^2} \right)^2 + 2\upsilon \left(\frac{\partial^2 W(x,y)}{\partial x^2} \right) \left(\frac{\partial^2 W(x,y)}{\partial y^2} \right) \right] - p(x)W(x,y) \tag{2}$$

and

$$C(x,y) = \frac{D(x,y)}{2} \left[2(1 - \upsilon) \left(\frac{\partial^2 W(x,y)}{\partial x \, \partial y} \right)^2 \right] \tag{3}$$

where

$$D(x,y) = \frac{E(x,y)\left(h(x,y)\right)^3}{12(1 - \nu^2)} \tag{3A}$$

Obtaining an exact solution to equation (1) is not a simple task. Therefore, an approximate solution will be used.

The energy integral U is evaluated approximately in terms of the unknown deflections at a finite number of points in the coordinate plane called grid points. Minimization of the resulting expression for U leads to a set of simultaneous equations involving the deflections at the grid points.

Grid points are located at the intersection of regular grid lines as shown in Figure 1. They are identified by numbering in any convenient order from 1 to NT.

In order to discuss the approximation and subsequent minimization of the energy integral, Figures 1 and 2 illustrate some notation relating to the grid points. About every central grid point where the unknown deflection, W, is to be calculated there is a cluster of grid points with subscripts showing their directional relationship to that central point. However, the directional subscripts are not limited to deflections alone. They are used to specify any values necessary in the discussion.

Expressing the energy in terms of the unknown deflections is accomplished in the following four steps:

(1) By use of finite-difference expressions, B(x,y) is evaluated at each grid point on the plate.

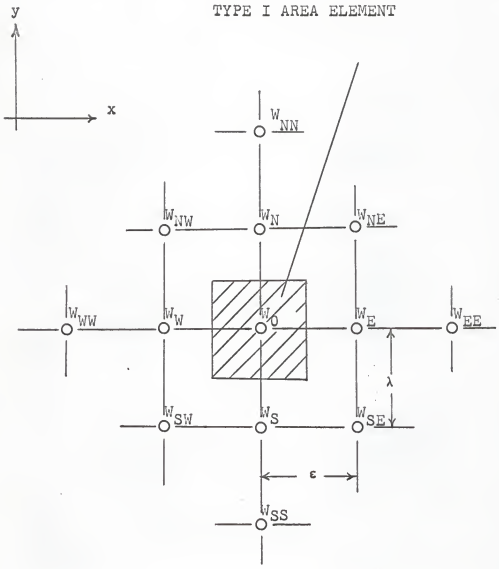

FIGURE 1. ILLUSTRATION OF A TYPE I AREA ELEMENT AND THE CORRESPONDING NOTATION USED IN THE APPROXIMATE INTEGRATION OF B(x,y)

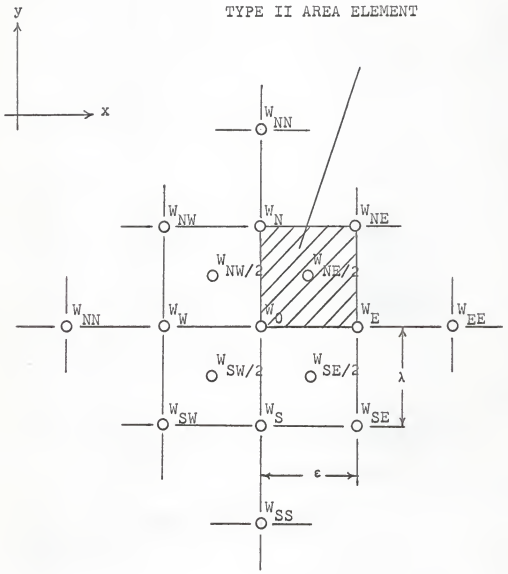

FIGURE 2. ILLUSTRATION OF A TYPE II AREA ELEMENT AND THE CORRESPONDING NOTATION USED IN THE APPROXIMATE INTEGRATIONS OF C(x,y). NOTE THAT HALF-STATION POINTS ARE USED.

(2) The values of $B(x,y)$ found in step (1) are used in a numerical integration to approximate the value of the first integral on the right in equation (1A).

(3) $C(x,y)$ is evaluated at half-stations but still is expressed in terms of deflections at the grid points.

(4) The values of $C(x,y)$ found in step (3) are used in a separate numerical integration to approximate the second integral in equation (1A).

The finite-difference expressions used are as follows:

$$\left[\frac{\partial^2 W(x,y)}{\partial x^2}\right]_0 = \frac{1}{\epsilon^2}\left[W_W - 2W_0 + W_E\right] \tag{4}$$

$$\left[\frac{\partial^2 W(x,y)}{\partial y^2}\right]_0 = \frac{1}{\lambda^2}\left[W_S - 2W_0 + W_N\right] \tag{5}$$

$$\left[\frac{\partial^2 W(x,y)}{\partial x\,\partial y}\right]_{NE/2} = \frac{1}{\epsilon\lambda}\left[W_{NE} - W_N - W_E + W_0\right] \tag{6}$$

Substituting expressions (4), (5), and (6) into equation (2) the value of $B(x,y)$ at a typical grid point would be

$$B_0 = \frac{D_0}{2}\left[\frac{1}{\epsilon^4}\left(W_W - 2W_0 + W_E\right)^2 \quad \frac{1}{\lambda^4}\left(W_S - 2W_0 + W_N\right)^2 + \frac{2\upsilon}{\epsilon^2\lambda^2}\left(W_W - 2W_0 + W_E\right)\left(W_S - 2W_0 + W_N\right)\right] - P_0 W_0$$

A typical value of C(x,y) would be

$$C_{NE/2} = \frac{D_{NE/2}}{2}\left[\frac{2(1-\upsilon)}{\varepsilon^2\lambda^2}\left(W_{NE} - W_N - W_E + W_0\right)^2\right]$$

At the edge of a plate, use of the finite-difference expressions (4), (5), and (6) involve grid points lying off the plate where W(x,y) has no meaning. This leads to the introduction of fictitious deflections at these off plate points just as though the deflection surface were smoothly extended. These fictitious deflections enter the energy approximation and are determined by minimization just the same as the deflections of the grid points on the plate.

In the approximate integration of B(x,y), each grid point on the plate is assigned an element of plate area. Figure 1 shows this type area designation (referred to as type 1 areas). The contribution to the potential energy from a type 1 area element is simply $U = \alpha\varepsilon\lambda B_0$ where $\alpha\varepsilon\lambda$ represents the area of the element. Integration of C(x,y) requires a separate area breakdown of the plate as shown in Figure 2 (referred to as type 2 areas). The contribution to the potential energy of this type area element is $\alpha_{NE/2}\varepsilon\lambda C_{NE/2}$.

When the results of the approximate integration of B(x,y) and C(x,y) are substituted into equation (1A), U appears as a function of the deflections at the grid points. Then by applying the principle of minimum potential energy, a set of NRR simultaneous equations evolve. These simultaneous equations can be

written in matrix form as

$$\left[S \right] \left\{ W \right\} = \varepsilon\lambda \left[\alpha p \right] \tag{7}$$

Thus far in the discussion no constraints have been placed on the plate; that is all points have been free to deflect. Now let us consider the case of a fixed edge where the boundary conditions $W(x,y) = 0$ and $\frac{\partial W(x,y)}{\partial x} = 0$ must be satisfied. To obtain zero deflections at a fixed edge all that need be done is to substitute zero deflection into the energy expressions for those grid points lying on that fixed edge. To simulate a zero slope at a fixed edge simply assign the grid point one interval inside the fixed edge the same deflection as the grid point one interval outside the fixed edge. This eliminates the off plate points at a fixed edge from the energy expressions. Off-plate points eliminated in this manner are commonly called image points.

After applying the edge conditions, minimization of the energy expressions proceeds as with the unconstrained plate and a set of simultaneous equations is obtained.

If the plate is undergoing unforced flexural oscillations, $W(x,y)$ can be considered the mode shape if $p(x,y)$ is replaced by the inertial load of the plate, $w^2\rho(x,y)W(x,y)$. If this substitution is made into equation (7) the following equation results.

$$\left[S \right] \left\{ W \right\} = \varepsilon\lambda w^2 \left[\alpha\rho \right] \left\{ W \right\} \tag{8}$$

Equation (8) is a characteristic-value, or eigenvalue, problem which can be solved for the natural frequencies and their corres-

ponding mode shapes. The method of solution used in this paper utilizes electronic computers. The computer programs used are shown in Appendix C.

APPLICATIONS

In a series of applications the method introduced by Houbolt (1) was used to approximate the natural frequencies and nodal patterns of four sets of cantilevered triangular variable-thickness plates. The planform and physical properties for each set are shown in Figure 3. As with most finite difference techniques, a fine grid point results in more accurate answers than a coarse one. Due to limitations on the size of computer available each plate in this study was divided into 28 finite areas. The plates were divided in such a way that the regularly spaced grid points are located at approximately the center of the areas. Walton (2) found that this arrangement of grid points was desirable from the point of view of accuracy of the resulting frequency calculations. Figures 6-9 (Appendix A) show the grid point location and corresponding area breakdown for each set of plates analyzed.

The thickness of a plate at any point is given by the equation $h(x) = h_o(1-T\frac{x}{L})$, where T is the taper ratio and L is the total length of the plate perpendicular to the fixed edge. For each planform five different taper ratios were used; namely 0.0, 0.2, 0.4, 0.6, and 0.8.

For identification purposes each plate is designated by a two character code. The first character designates the planform and the second character represents ten times the taper ratio. For example, a plate having planform B and a taper ratio of 0.6 would be identified as plate B-6.

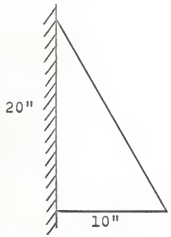

(a) Planform A

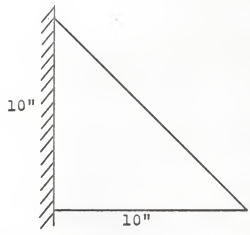

(b) Planform B

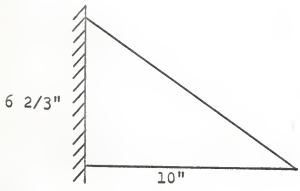

(c) Planform C

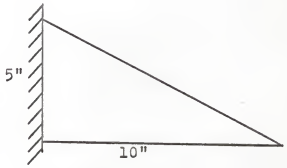

(d) Planform D

$E = 30 \times 10^6$ psi

$\upsilon = 0.250$

$h_0 = 0.061$" (thickness at fixed edge)

FIGURE 3. PLANFORMS OF THE TRIANGULAR PLATES ANALYZED

PRESENTATION AND DISCUSSION OF RESULTS

The results of applications made in this investigation are presented in Tables 1, 2, and 3 and in Figures 4-5 and 10-27. Tables 1 and 2 and Figures 4 and 5 are presented to show the accuracy of the method used in this analysis.

In Table 1 a comparison is made between computed and experimental values for the frequencies of the first five modes of vibration of triangular plates. It is seen that, in general, computed values compare well with experimental values.

TABLE 1

EXPERIMENTAL PLATE NATURAL FREQUENCIES
COMPARED WITH COMPUTED VALUES

PLATE	MODE	NATURAL FREQUENCIES (CPS)	
		EXPERIMENTAL (6)	COMPUTED
A - 0	1	32.8	32.4
	2	91	90
	3	164	164
	4	181	175
	5	283	263
B - 0	1	34.5	36.3
	2	136	139
	3	190	192
	4	325	326
	5	441	431

Table 2 shows a comparison between two sets of computed values for the frequency of the first mode of vibration of a set of variable thickness square plates simply-supported on all sides. The results found by Houbolt's method shown in this table were obtained only as a means of checking the computer programs written by the author and are not the main interest of this study. The results computed by Houbolt's method compare very favorably with those found by Appl and Byers (3) using a bounding technique.

TABLE 2

COMPARISON OF VALUES OF THE FUNDAMENTAL EIGENVALUE OF SQUARE SIMPLY-SUPPORTED PLATES WITH A LINEAR THICKNESS VARIATION

TAPER RATIO	EIGENVALUE (K) FOUND BY HOUBOLTS METHOD (1)	EIGENVALUE (K') FOUND BY APPL AND BYERS (3)	$\frac{K}{K'}$
0.0	376.7	389.6	.967
0.2	455.0	470.5	.967
0.4	538.8	557.2	.967
0.6	528.2	650.1	.966
0.8	724.3	748.2	.968

* The eigenvalues K and K' are related to the natural frequency by the following equation

$$K = K' = \frac{(2\pi f)^2 a^4 \rho_r}{D_r}$$

where "a" is the length of the plate.

A term of the form f_{ij} is used in the discussion of results. Some explanation of this term is necessary. The f represents a frequency, as described in the list of symbols, while the subscripts i and j identify the frequency as belonging to a particular mode of vibration of a certain type of plate. The i signifies which mode of vibration and the j signifies the taper ratio. Thus f_{36} represents the frequency of the third mode of vibration of a plate having a taper ratio of 0.6.

Nodal patterns for each plate were computed as another means of checking results. In the process of calculating the eigenvalues the eigenvectors were also calculated. The nodal patterns were then obtained from the eigenvectors, i.e. mode shapes, by linear interpolation between the grid points. These interpolated nodal patterns are shown in Figures 4 and 5 of the presentation of results and Figures 10-28 shown in Appendix B. A comparison between experimental nodal patterns and computed nodal patterns is shown for plates A-0 and B-0 in Figures 4 and 5.

The results shown in Table 3 (a) are the computed frequencies for plates having planform A. The corresponding nodal patterns are shown in Figures 4 and 10-13.

It can be seen from the table that the taper ratio has little effect on the magnitude of the frequency of the first mode of vibration until the taper ratio exceeds 0.6. This is indicated by the fact that the total increase in the magnitude of the frequency of the first mode between taper ratios of 0.0 and 0.6 is less than 5% while an increase of approximately 10% is shown between taper ratios of 0.6 and 0.8.

TABLE 3

COMPUTED FREQUENCIES FOR TRIANGULAR PLATES

PLATE	FREQUENCY (CPS)				
	1	2	3	4	5
A - 0	32.4	90	164	175	263
A - 2	32.7	87	154	166	245
A - 4	33.1	84	144	156	226
A - 6	33.8	81	133	146	206
A - 8	38.1	72	106	119	160

(a)

PLATE	FREQUENCY (CPS)				
	1	2	3	4	5
B - 0	36.3	139	192	326	431
B - 2	36.8	133	184	305	402
B - 4	37.5	126	176	281	374
B - 6	38.3	119	167	255	338
B - 8	43.0	99	148	187	252

(b)

TABLE 3 (cont.)

PLATE	FREQUENCY (CPS)				
	1	2	3	4	5
C - 0	38.2	159	239	376	554
C - 2	38.7	150	232	348	520
C - 4	39.6	142	227	319	488
C - 6	40.6	132	219	287	444
C - 8	45.7	109	193	213	319

(c)

PLATE	FREQUENCY (CPS)				
	1	2	3	4	5
D - 0	39.1	165	295	389	655
D - 2	39.7	156	289	360	606
D - 4	40.7	147	286	331	551
D - 6	41.8	136	274	299	488
D - 8	47.2	114	208	261	335

(d)

As was the case with the frequencies of the first mode the taper ratio of the plate has little effect on the higher frequencies of the second through fifth modes if the ratio does not exceed 0.6. The differences between f_{20} and f_{22}, f_{22} and f_{24}, f_{24} and f_{26} are 3-4% respectively while an increase of 9-10% results between f_{26} and f_{28}. This same trend is seen in the frequencies of modes 3, 4, and 5.

The pattern established by the frequencies of the first mode of vibration is distinct from that of the frequencies of higher modes. An increase in magnitude is shown in the frequency of the first mode as the taper ratio increases while a corresponding decrease in frequency is shown in modes two through five. This increase in frequencies of the first mode was somewhat unexpected. At first it was thought that computer round-off might be the cause of this phenomena. However, after recomputing some of the solutions using a different number of significant digits, it was found that the results were the same to three significant figures and therefore the round-off error explanation was discarded.

The pattern taken by the frequency of the first mode is not restricted to the A-series alone. It occurs for series B, C, and D as well.

In Figure 4 experimental nodal patterns are plotted along with the computed nodal patterns for the uniform-thickness plate A-0. Good agreement is shown between these two patterns.

Figures 10-13 show the computed nodal patterns for plates A-2, A-4, A-6, and A-8, respectively. The taper ratio has small effect on the nodal patterns in that there is very little difference between the nodal patterns of the uniform thickness

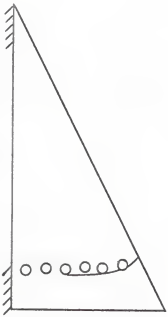

(a) Calculated nodes for mode 2

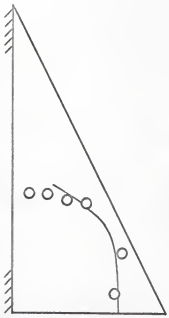

(b) Calculated nodes for mode 3

—— Experimental (6)

O Computed

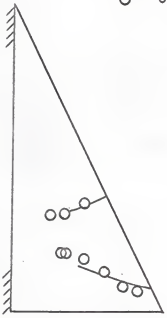

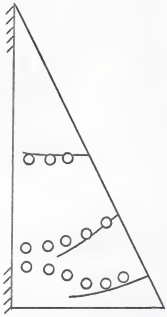

FIGURE 4. NODAL PATTERNS FOR PLATE A-0

and those of the variable-thickness plates.

Table 3 (b) shows the computed frequencies for the B series plates. Their corresponding nodal pattern are shown in Figures 5 and 14-17.

The computed frequencies for the B-series follow the same general pattern as those of the A-series. Again, the taper ratio has a small effect on the magnitude of the frequencies of the various modes of vibration until it exceeds 0.6. The difference between the frequencies then becomes more pronounced. It should be noted that the frequencies of the third and fourth modes tend to approach one another as the taper ratio increases. The difference between f_{30} and f_{40} is 134 cps while the corresponding difference between f_{38} and f_{48} is only 40 cps. This convergence will be discussed further in connection with the plates of the C and D series.

In Figure 5, experimental nodal patterns are plotted along with the computed patterns for plate B-0. The agreement between these two sets of patterns is quite good. Nodal patterns for the variable-thickness plates of the B-series, Figures 14-17, show only slight variation from those in Figure 5 for the uniform-thickness plate. The only noticeable variation that does occur is in mode 3. As the taper ratio increases the third mode seems to become more of a tranverse mode.

The computed frequencies for the C-series plates are shown in Table 3 (c). Their corresponding nodal patterns are shown in Figures 18-22.

(a) Calculated nodes for mode 2

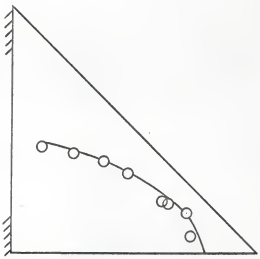

(b) Calculated nodes for mode 3

— Experimental (6)

○ Computed

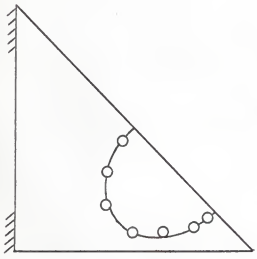

(c) Calculated nodes for mode 4

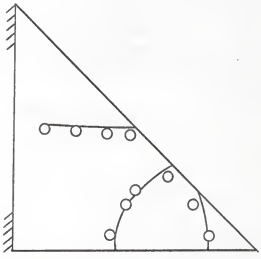

(d) Calculated nodes for mode 5

FIGURE 5. NODAL PATTERNS FOR PLATE B-0

The computed frequencies display patterns almost identical to those of the B-series plates. However, the convergence of the third and fourth modes is more pronounced for the C-series plates. In fact, they converge to within 20 cps for the C-8 plate.

The nodal patterns also show a definite change for this plate. Modes 3 and 4 seem to interchange. That is, mode 3 seems to change from a primarily transverse mode to a primarily longitudinal mode while mode 4 changes from a primarily longitudinal mode to a primarily transverse mode.

The computed results for the D-series plates, Table 3 (d), follow the same general pattern as those of the C-series. The convergence of the frequencies of the third and fourth mode which occurred in the C-series occurs in the D-series as well, the difference between f_{36} and f_{46} is only 25 cps. For plate D-4, f_{34} and f_{44} differ by 45 cps and for plate D-8, f_{38} and f_{48} differ by 53 cps. That is, the difference between the frequencies of modes 3 and 4 converge to a minimum at a taper ratio somewhere around that of the D-6 plate.

From the nodal patterns, Figures 23-27, it is seen that a change occurs between the D-6 plate and the D-8 plate. As was the case with the C-8 plate, the third and fourth modes seem to interchange. For the D-6 plate, mode 3 is primarily a transverse mode while mode 4 represents primarily a longitudinal mode. For the D-8 plate, however, mode 3 is primarily a longitudinal mode while mode 4 becomes primarily a transverse mode. Thus it is seen that the nodal patterns and the computed frequencies agree in that changes occur in both at approximately the same taper ratio for both the C and D series of plates.

CONCLUSIONS

In this study of the natural frequencies of tapered triangular plates, calculations were made for a series of plates having varying taper ratios. Computed values for the first five natural frequencies and nodal patterns were obtained. By comparing some of these frequencies and nodal patterns with those found previously in other investigations it was found that Houbolt's method is well adapted to computing the frequency of vibration for the first five modes of vibration for tapered, triangular plates.

It was also found that the taper ratio has very little effect on the magnitude of the frequencies of the first five modes of vibration if it is kept equal to, or less than, 0.6. The nodal patterns have the same trend in that small variations result if the taper ratio does not exceed 0.6. When a taper ratio of 0.8 was used an exchange in nodal patterns occurs for the C and D series plates.

Houbolt's method of analysis is quite versatile in that it can be applied to problems having any planform or taper ratio as well as to those having various boundary conditions. The fact that the solution can be completely computerized is of greatest importance. With the present and increasing capability of electronic computers, there is almost no limit to the size of problem which can be solved.

SUGGESTIONS FOR FURTHER RESEARCH

Further research with the natural vibrations problem connected with thin plates is needed in many areas. Among these areas are plates with longitudinal stiffeners, plates with holes in them, and sandwich plates.

Houbolt's method of analysis should be directly applicable to plates having lateral stiffeners and to plates having holes in them. To solve the sandwich plate problem, however, a certain amount of modification would have to be made to Houbolt's method. Research in all three of these areas is suggested.

Experimental work with the triangular tapered plates analyzed in this study by Houbolt's method is needed to supplement the computed results for the natural frequencies and nodal patterns.

LIST OF SYMBOLS

A - Area of middle surface of plate

$B(x,y)$ - Part of potential energy (See eq. 2)

$C(x,y)$ - Part of potential energy (See eq. 3)

$D(x,y)$ - Flexural rigidity of plate (See eq. 3A)

$E(x,y)$ - Young's modulus of elasticity

$h(x,y)$ - Plate thickness

K - Number of grid points at which load is finite

$p(x,y)$ - Load per unit area of plate

NRR - Number of unknown deflections in the energy expressions after conditions of constraint have been applied

NT - Total number of grid points

U - Total potential energy of the plate

$W(x,y)$ - Bending deflections of plate

x,y - Cartesian coordinates

α - Area weighting factor (unity for any rectangular area in dimension)

ε - Horizontal distance between grid lines

λ - Vertical distance between grid lines

υ - Poisson's ratio

$\rho(x,y)$ - Mass of plate per unit area

w - Eigenvalue found by computer

f - Frequency in cycles per second

ρ_r - Reference value for the mass per unit area of plate

D_r - Reference value for plate rigidity

Matrices:

$[s]$ - Square matrix NRR x NRR in dimension resulting from minimization of energy expressions

$\{\}$ - Any column matrix

ACKNOWLEDGMENT

I wish to express my sincere appreciation for the direction and guidance given by Dr. Robert R. Snell, Associate Professor of Civil Engineering at Kansas State University. Without his efforts this research would not have been possible.

For his valuable suggestions in the organization and review of this thesis, I would like to extend my sincere thanks to Dr. Jack B. Blackburn, Head of the Civil Engineering Department at Kansas State University.

BIBLIOGRAPHY

1. Houbolt, John C., "A Study of Several Aerothermoelastic Problems of Aircraft Structures in High-speed Flight," Nr. 5, Mitteilungen aus dem Institut fur Flugzeugstatik und Leichtbau. Leemann (Zurich), C. 1958.

2. Walton, William C., "Applications of a General Finite-Difference Method for Calculating Bending Deformations of Solid Plates," National Aeronautics and Space Administration, Technical Note D-536, C. 1958.

3. Appl, F. C. and Byers, N. R., "Bounds for the Fundamental Frequency of a Tapered Plate," Journal of Applied Mechanics, 1964.

4. Barton, M. V., "Vibrations of Rectangular and Skew Cantilever Plates," Journal of Applied Mechanics, Vol. 18, Nr. 2, June, 1951.

5. Dalley, J. W. and Ripperger, E. A., "Experimental Values of Natural Frequencies for Skew and Rectangular Cantilever Plates," Society for Experimental Stress Analysis, Proceedings, Vol. 7, Nr. 2, 1952.

6. Gustafson, P. N., Stokey, W. F., and Zorowski, C. F., "An Experimental Study of Natural Vibrations of Cantilevered Triangular Plates," Journal of Aeronautical Sciences, Vol. 20, Nr. 5, May, 1953.

APPENDIX A

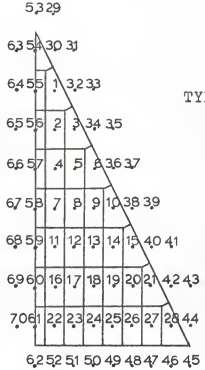

TYPE I AREA BREAKDOWN

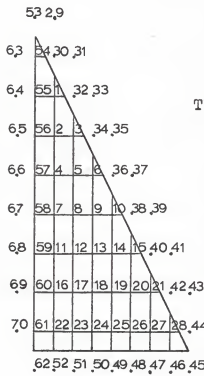

TYPE II AREA BREAKDOWN

FIGURE 6. GRID POINT LOCATIONS AND AREA BREAKDOWNS FOR PLATE A

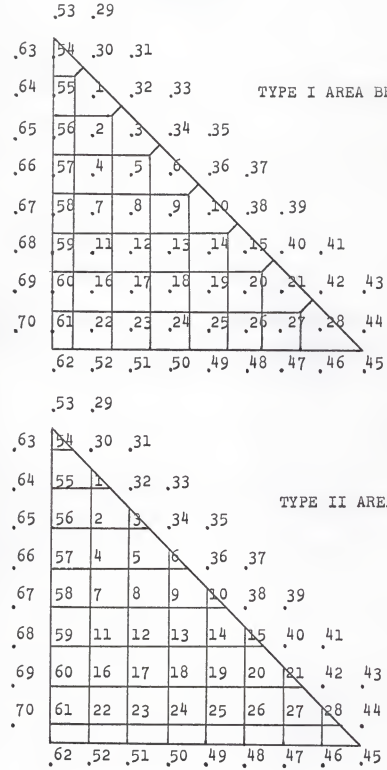

FIGURE 7. GRID POINT LOCATIONS AND AREA BREAKDOWNS FOR PLATE B

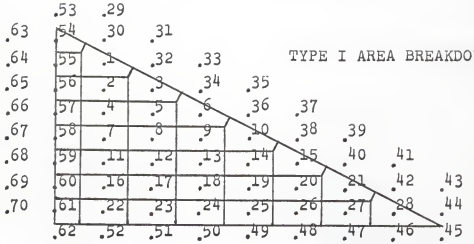

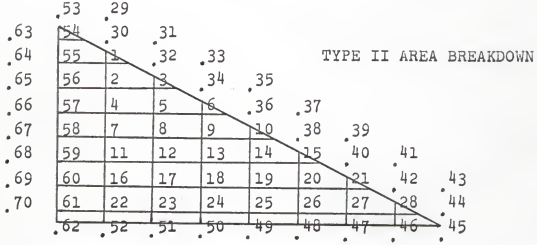

FIGURE 8. GRID POINT LOCATIONS AND AREA BREAKDOWNS FOR PLATE C

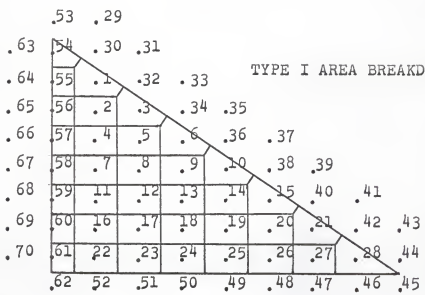

TYPE I AREA BREAKDOWN

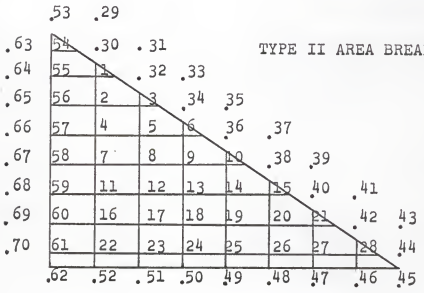

TYPE II AREA BREAKDOWN

FIGURE 9. GRID POINT LOCATIONS AND AREA BREAKDOWNS FOR PLATE D

APPENDIX B

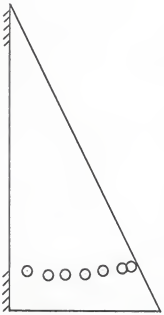

(a) Calculated nodes for mode 2

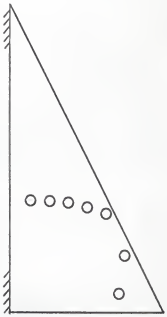

(b) Calculated nodes for mode 3

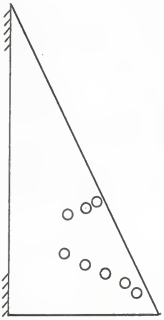

(c) Calculated nodes for mode 4

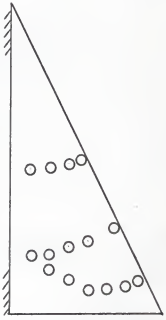

(d) Calculated nodes for mode 5

FIGURE 10. NODAL PATTERNS FOR PLATE A-2

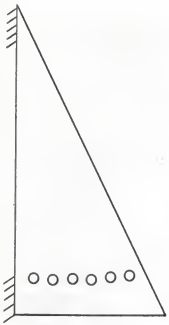

(a) Calculated nodes for mode 2

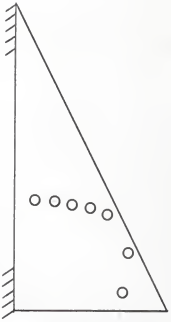

(b) Calculated nodes for mode 3

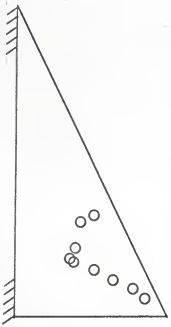

(c) Calculated nodes for mode 4

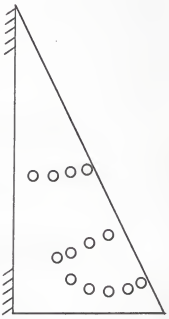

(d) Calculated nodes for mode 5

FIGURE 11. NODAL PATTERNS FOR PLATE A-4

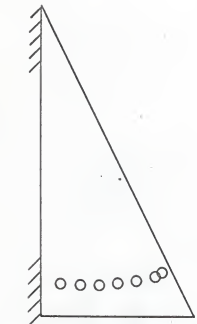

(a) Calculated nodes for mode 2

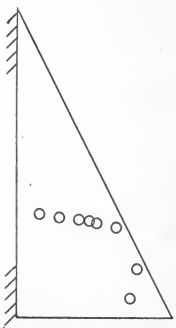

(b) Calculated nodes for mode 3

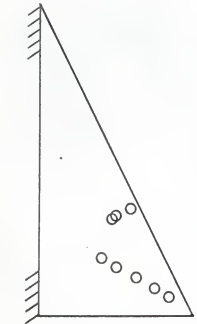

(c) Calculated nodes for mode 4

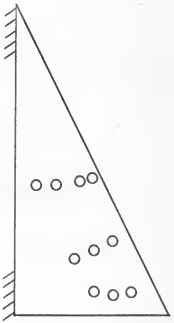

(d) Calculated nodes for mode 5

FIGURE 12. NODAL PATTERNS FOR PLATE A-6

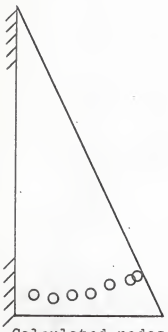

(a) Calculated nodes for mode 2

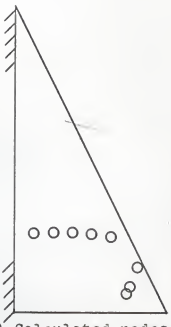

(b) Calculated nodes for mode 3

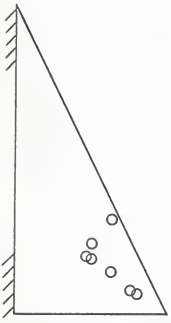

(c) Calculated nodes for mode 4

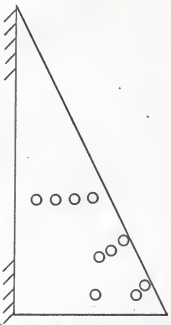

(d) Calculated nodes for mode 5

FIGURE 13. NODAL PATTERNS FOR PLATE A-8

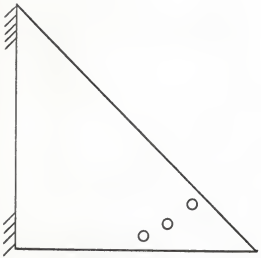

(a) Calculated nodes for mode 2

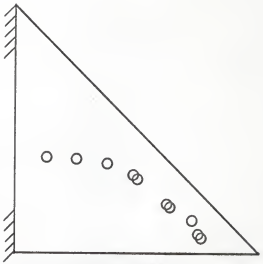

(b) Calculated nodes for mode 3

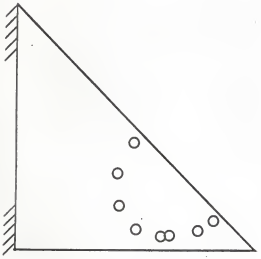

(c) Calculated nodes for mode 4

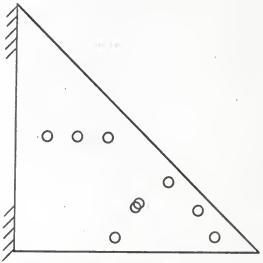

(d) Calculated nodes for mode 5

FIGURE 14. NODAL PATTERNS FOR PLATE B-2

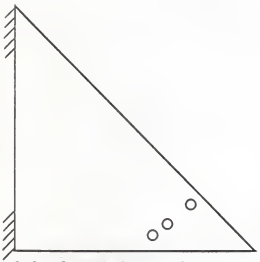

(a) Calculated nodes for mode 2

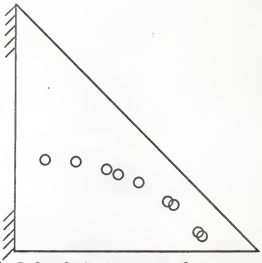

(b) Calculated nodes for mode 3

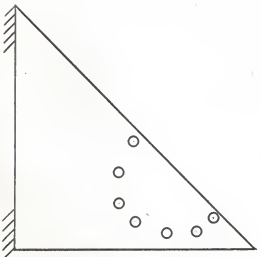

(c) Calculated nodes for mode 4

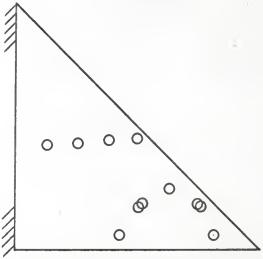

(d) Calculated nodes for mode 5

FIGURE 15. NODAL PATTERNS FOR PLATE B-4

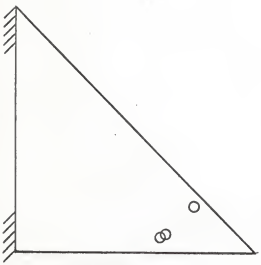

(a) Calculated nodes for mode 2

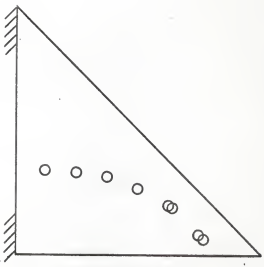

(b) Calculated nodes for mode 3

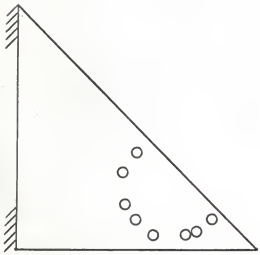

(c) Calculated nodes for mode 4

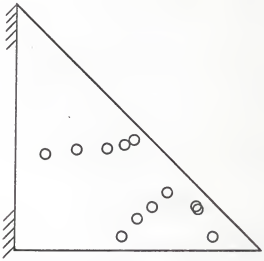

(d) Calculated nodes for mode 5

FIGURE 16. NODAL PATTERNS FOR PLATE B-6

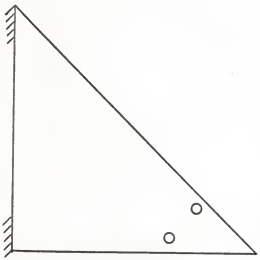

(a) Calculated nodes for mode 2

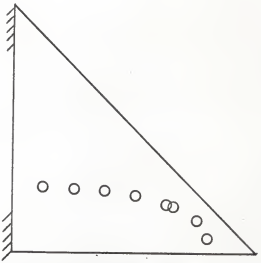

(b) Calculated nodes for mode 3

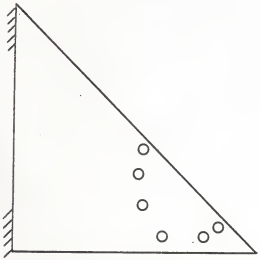

(c) Calculated nodes for mode 4

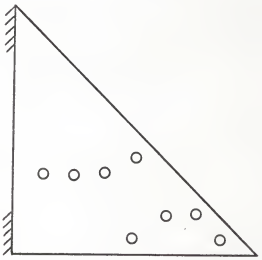

(d) Calculated nodes for mode 5

FIGURE 17. NODAL PATTERNS FOR PLATE B-8

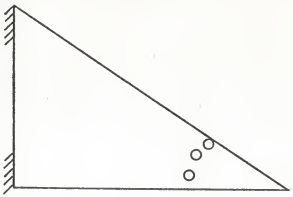

(a) Calculated nodes for mode 2

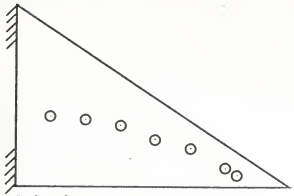

(b) Calculated nodes for mode 3

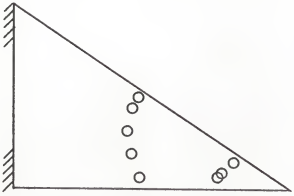

(c) Calculated nodes for mode 4

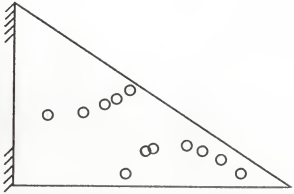

(d) Calculated nodes for mode 5

FIGURE 18. NODAL PATTERNS FOR PLATE C-0

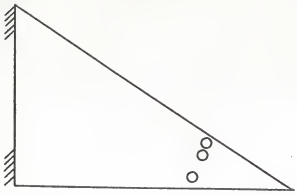

(a) Calculated nodes for mode 2

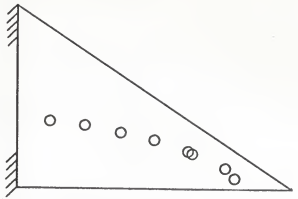

(b) Calculated nodes for mode 3

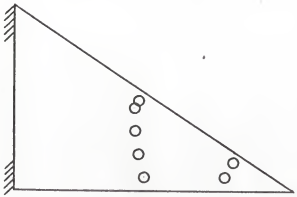

(c) Calculated nodes for mode 4

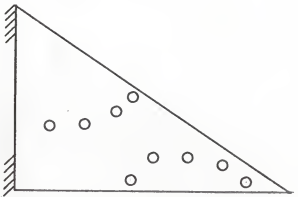

(d) Calculated nodes for mode 5

FIGURE 19. NODAL PATTERNS FOR PLATE C-2

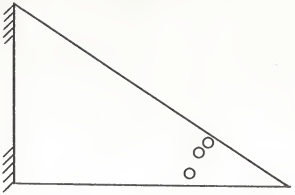

(a) Calculated nodes for mode 2

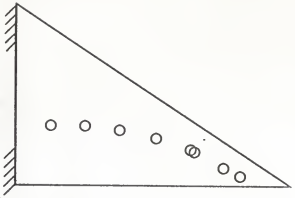

(b) Calculated nodes for mode 3

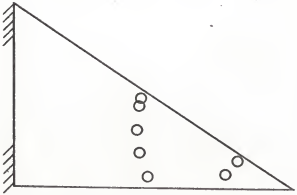

(c) Calculated nodes for mode 4

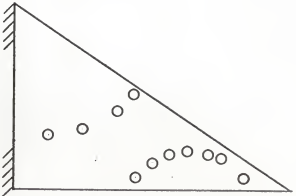

(d) Calculated nodes for mode 5

FIGURE 20. NODAL PATTERNS FOR PLATE C-4

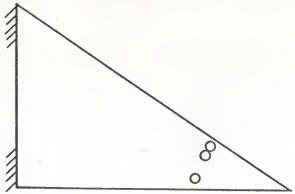

(a) Calculated nodes for mode 2

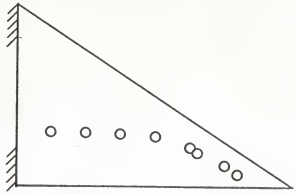

(b) Calculated nodes for mode 3

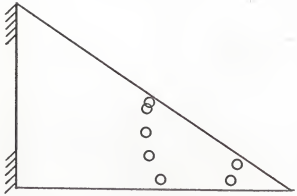

(c) Calculated nodes for mode 4

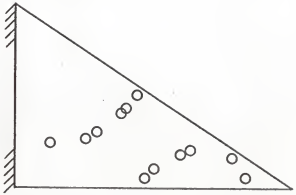

(d) Calculated nodes for mode 5

FIGURE 21. NODAL PATTERNS FOR PLATE C-6

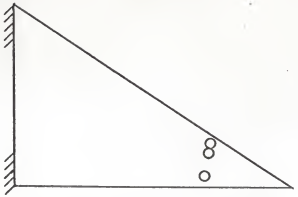

(a) Calculated nodes for mode 2

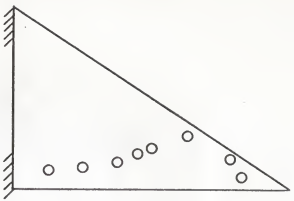

(b) Calculated nodes for mode 3

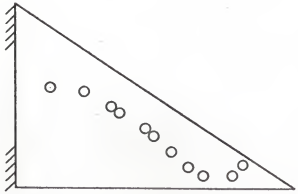

(c) Calculated nodes for mode 4

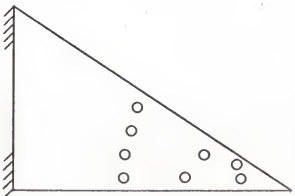

(d) Calculated nodes for mode 5

FIGURE 22. NODAL PATTERNS FOR PLATE C-8

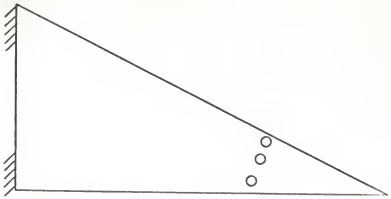

(a) Calculated nodes for mode 2

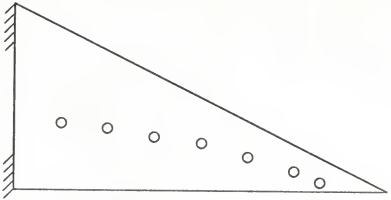

(b) Calculated nodes for mode 3

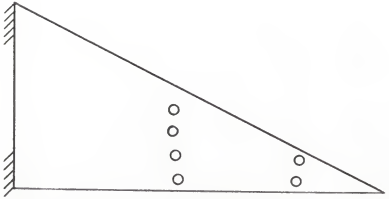

(c) Calculated nodes for mode 4

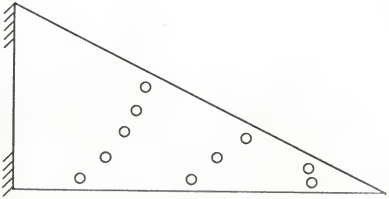

(d) Calculated nodes for mode 5

FIGURE 23. NODAL PATTERNS FOR PLATE D-0

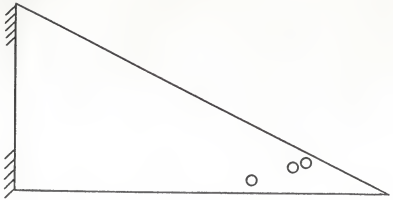

(a) Calculated nodes for mode 2

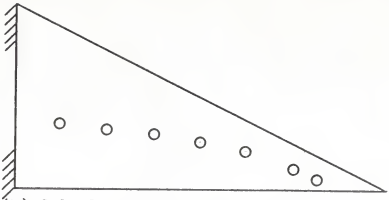

(b) Calculated nodes for mode 3

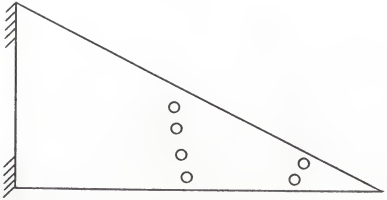

(c) Calculated nodes for mode 4

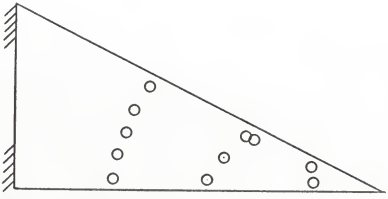

(d) Calculated nodes for mode 5

FIGURE 24. NODAL PATTERNS FOR PLATE D-2

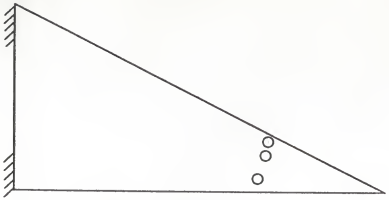

(a) Calculated nodes for mode 2

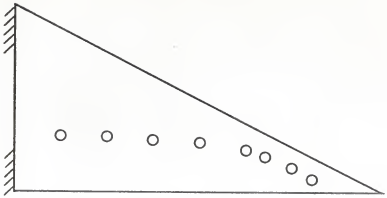

(b) Calculated nodes for mode 3

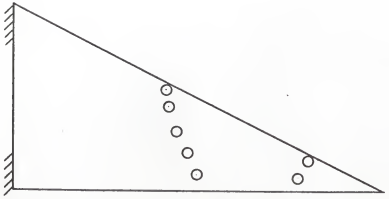

(c) Calculated nodes for mode 4

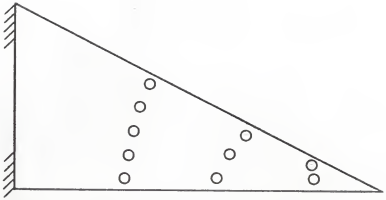

(d) Calculated nodes for mode 5

FIGURE 25. NODAL PATTERNS FOR PLATE D-4

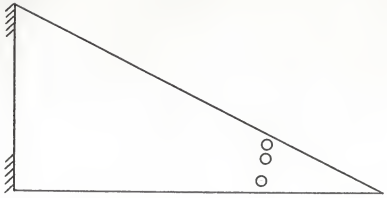

(a) Calculated nodes for mode 2

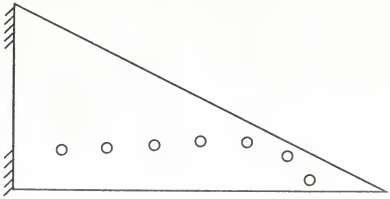

(b) Calculated nodes for mode 3

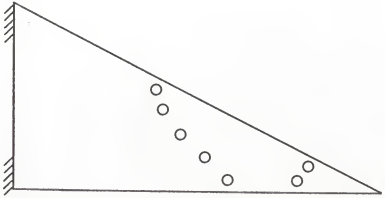

(c) Calculated nodes for mode 4

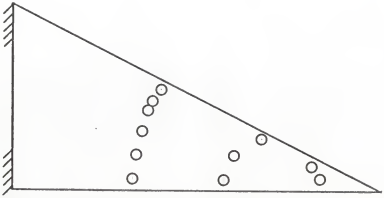

(d) Calculated nodes for mode 5

FIGURE 26. NODAL PATTERNS FOR PLATE D-6

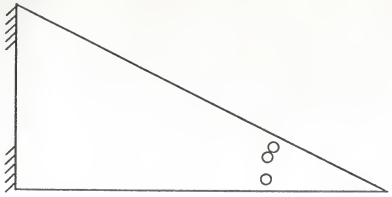

(a) Calculated nodes for mode 2

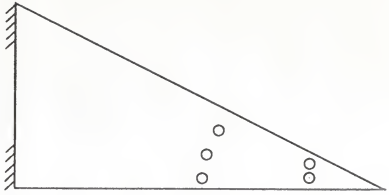

(b) Calculated nodes for mode 3

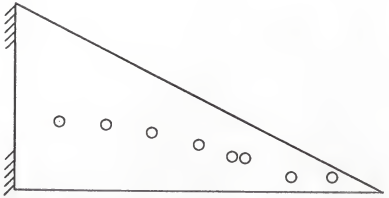

(c) Calculated nodes for mode 4

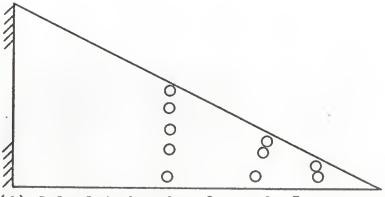

(d) Calculated nodes for mode 5

FIGURE 27. NODAL PATTERNS FOR PLATE D-8

APPENDIX C

DISCUSSION OF COMPUTER PROGRAMS

Due to limitations on the size of computers available, the computer solution to the vibrations problem was broken down into two programs. The first program solves for the coefficients of the simultaneous equations resulting from the minimization of the energy expression. This program is written for the IBM 1620 computer with 60,000 core storage locations. It takes about 5-7 minutes of actual computer time to solve for the coefficients of a 28 x 28 set of equations as was used with the triangular plates.

The second program takes the set of coefficients found by program 1 and proceeds to find the eigenvalues and eigenvectors. This program is written for an IBM 1410 computer and requires 60-75 minutes to solve for the eigenvalues and eigenvectors. These eigenvalues are related to the natural frequencies by the following equation.

$$w = \frac{2\varepsilon^4(2\Pi f)^2\rho_r}{D_r}$$

where w is the eigenvalue found in the computer solution.

The corresponding eigenvectors found in the computer solution are an approximation to the mode shapes.

An example set of input data and output results are shown.

LIST OF SYMBOLS FOR PROGRAMS 1 AND 2

NRR - Number of unknown deflections in the energy expressions after conditions of constraint have been applied

K - Number of grid points at which load is finite

LL - NRR - K

NT - Total number of grid points

U - Poisson's ratio

EOL - ϵ/λ - Ratio of horizontal distance between grid points to vertical distance between grid points

N(I) - Number of the central grid point

A(I) - Type 1 area element for grid point "I"

AA(I) - Type 2 area element for grid point "I"

T(I) - Thickness at centroid of type I area at grid point "I"

TT(I) - Thickness at centroid of type II area at grid point "I"

NE(I), NEE(I), NSE(I), . . . NW(I) - Directional grid point locations from grid point "I"

S - Total coefficient matrix = $\begin{bmatrix} S1 & S2 \\ S2^T & S3 \end{bmatrix}$

S1 - K x K Symetric matrix

S2 - K x LL Matrix

$S2^T$ - Transpose of S2

S3 - LL x LL Symetric matrix

FLOW DIAGRAM FOR PROGRAM 1

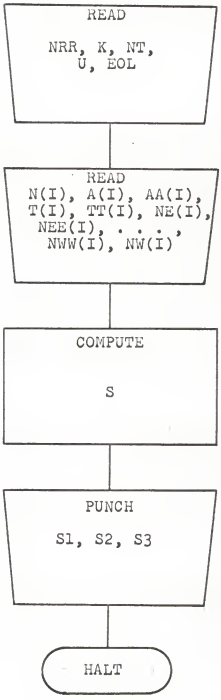

```
      PROGRAM 1      CALCULATION OF COEFFICIENT MATRIX
    DIMENSION N(75),NNN(75),NNW(75),NN(75),NNE(75),NWW(75)
    DIMENSION NE(75),NEE(75),NSE(75),NS(75),NSW(75),NSS(75)
    DIMENSION AA(75),T(75),TT(75),S(75),D(75),DD(75)
    DIMENSION S2(30,30),S3(30,30),TIMES(36),NW(75),A(75)
100 READ 1, U,ECL,NRR,K,NT
  1 FORMAT(2F5.3,3I3)
    LLLN=0
    PUNCH 444, NRR,K
444 FORMAT(I3,I3)
    L=NRR-K
    READ 2, (N(I),A(I),AA(I),T(I-,TT(I),NE(I),NEE(I),NSE(I)
   1,NS(I),NSW(I),NSS(I),NNN(I),NNW(I),NN(I),NNE(I),NWW(I),
   2NW(I),I=1,NT)
  2 FORMAT(I3,4F6.3,12I3)
    DO 555 I=1,K
    TIMES(I)= 1./(SQRTF(A(I)*T(I)))
555 CONTINUE
    IF(NRR-K)111,876,877
877 PUNCH 40, (TIMES(I),I=1,K)
876 DO 3 I=1,NT
    D(I)=A(I)*(T(I)**3)
    DD(I)=AA(I) *(TT(I)**3)
  3 CONTINUE
    E1=ECL
    E2=ECL**2
    E4=ECL**4
    IF(NRR -K)111,379,378
379 MJKL=K
    GO TO 377
378 MJKL=NRR
377 DO 4 I=1,MJKL
    A1=0.0
    A2=0.0
    A3=0.0
    A4=0.0
    A5=0.0
    A6=0.0
    A7=0.0
    A8=0.0
    A9=0.0
    A10=0.0
    A11=0.0
    A12=0.0
    AA1=0.0
    AA2=0.0
    AA3=0.0
    AA4=0.0
    AA5=0.0
    AA6=0.0
```

```
      AA7=0.0
      AA8=0.0
      AA9=0.0
      AA10=0.0
      AA11=0.0
      AA12=0.0
      DO 89 J=1,NRR
      S(J)=0.0
   89   CONTINUE
      K1=NNN(I)
      K2=NNW(I)
      K3=NN(I)
      K4=NNE(I)
      K5=NWW(I)
      K6=NW(I)
      K7=NE(I)
      K8=NEE(I)
      K9=NSE(I)
      K10=NS(I)
      K11=NSW(I)
      K12=NSS(I)
      IF(K1)111,56,55
   55 A1=D(K1)
      AA1=DD(K1)
      GO TO 57
   56 A1=0.0
      AA1=0.0
   57 IF(K2)111,58,59
   59 A2=D(K2)
      AA2=DD(K2)
      GO TO 60
   58 A2=0.0
      AA2=0.0
   60 IF(K3)111,61,62
   62 A3=D(K3)
      AA3=DD(K3)
      GO TO 63
   61 A3=0.0
      AA3=0.0
   63 IF(K4)111,64,65
   65 A4=D(K4)
      AA4=DD(K4)
      GO TO 67
   64 A4=0.0
      AA4=0.0
   67 IF(K5)111,68,69
   69 A5=D(K5)
      AA5=DD(K5)
      GO TO 80
   68 A5=0.0
      AA5=0.0
```

```
 80 IF(K6)111,81,82
 82 A6=D(K6)
    AA6=DD(K6)
    GO TO 83
 81 A6=0.0
    AA6=0.0
 83 IF(K7)111,84,85
 85 A7=D(K7)
    AA7=DD(K7)
    GO TO 86
 84 A7=0.0
    AA7=0.0
 86 IF(K8)111,107,108
108 A8=D(K8)
    AA8=DD(K8)
    GO TO 109
107 A8=0.0
    AA8=0.0
109 IF(K9)111,110,121
121 A9=D(K9)
    AA9=DD(K9)
    GO TO 122
110 A9=0.0
    AA9=0.0
122 IF(K10)111,123,124
124 A10=D(K10)
    AA10=DD(K10)
    GO TO 125
123 A10=0.0
    A10=0.0
125 IF(K11)111,126,127
127 A11=D(K11)
    AA11=DD(K11)
    GO TO 128
126 A11=0.0
    AA11=0.0
128 IF(K12)111,129,130
130 A12=D(K12)
    AA12=DD(K12)
    GO TO 28
129 A12=0.0
    AA12=0.0
 28 IF(K1)5,6,41
 41 IF(K1-NRR)5,5,6
  5 S(  K1)= 2.*E4*A3
  6 IF(K2)7,8,42
 42 IF(K2-NRR)7,7,8
  7 S(  K2)=2.*U*E2*(A6+A3)+4.*(1.-U)*E2*AA6
  8 IF(K3)9,10,43
 43 IF(K3-NRR)9,9,10
```

```
  9 S(  K3)=-4.*(E4+U*E2)*(D(I)+A3)-4.*(1.-U)*E2*(DD(I)+AA6)
 10 IF(K4)12,12,44
 44 IF(K4-NRR)11,11,12
 11 S(  K4)=2.*U*E2*(A7+A3)+4.*(1.-U)*E2*DD(I)
 12 IF(K5)13,14,45
 45 IF(K5-NRR)13,13,14
 13 S(  K5)=2.*A6
 14 IF(K6)15,16,46
 46 IF(K6-NRR)15,15,16
 15 S(  K6)=-4.*(1.+U*E2)*(A6+D(9))-4.*(1.-U)*(AA6+AA11)*E2
 16 Y=2.*(E4*(A3+4.*D(I)+A10))
    Z=4.*(1.-U)*E2*(DD(I)+AA6+ A111+ AA10)
    S(  I)=2.*A6+8.*D(I)+2.*A7+Y+16.*U*E2*D(I)+Z
    IF(K7)17,18,47
 47 IF(K7-NRR)17,17,18
 17 S(K7)=-4.*(1.+U*E2)*(D(I)+A7--4.*(1.-U)*E2*(DD(I)+AA10)
 18 IF(K8)19,20,48
 48 IF(K8-NRR)19,19,20
 19 S(  K8)=2.*A7
 20 IF(K11)21,22,49
 49 IF(K11-NRR)21,21,22
 21 S(  K11)=  2.*U*E2*(A6+A10)+4.*(1.-U)*E2*AA11
 22 IF(K10)23,24,34
 34 IF(K10-NRR)23,23,24
 23 S(  K10)=-4.*(E4+U*E2)*(D(I)+ A10)-4.*(1.-U)*E2*(AA10+
   1AA11)
 24 IF(K9)25,26,35
 35 IF(K9-NRR)25,25,26
 25 S(  K9)=2.*U*E2*(A7+A10)+4.*(1.-U)*E2*AA10
 26 IF(K12)37,37,36
 36 IF(K12-NRR)27,27,37
 27 S(  K12)=2.*E4*A10
 37 IF(I-K)773,773,224
773 IF(NRR-K)111,567,221
567 LLLN=LLLN+1
    DO 729 IJK=1,K
    S(IJK)=S(IJK)*TIMES(LLLN)*TIMES(IJK)
729 CONTINUE
    PUNCH 40, (S(III),III=1,K)
    GO TO 4
221 PUNCH 40, (S(III), III=1,K)
    DO 222 JJJ=1,L
    KKK=K+JJJ
    S2(I,JJJ)=S(KKK)
222 CONTINUE
    GO TO  4
224 DO 223 JJJ=1,L
    KKK=K+JJJ
    LLL=I-K
    S3(LLL,JJJ)=S(KKK)
223 CONTINUE
```

```
  4 CONTINUE
    PUNCH 880
880 FORMAT(12H+++++++++ ++)
 40 FORMAT(6E13.6)
    IF(NRR-K)100,100,376
376 PUNCH40,((S2(I,J),J=1,L),I=1,K)
    PUNCH 40, ((S3(I,J),J=1,L),I=1,L)
    GO TO 100
111 STOP
    END
```

FLOW DIAGRAM FOR PROGRAM 2

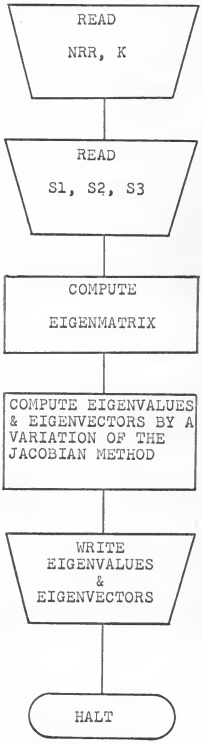

```
      PROGRAM 2  SOLVES FOR EIGENVALUES AND EIGENVECTORS
   MON$$      JOB
   MON$$      COMT 15,10,PAGES,,DILLAS KOERNER  CIVIL ENGG
   MON$$      ASGN MJB,12
   MON$$      ASGN MGO,16
   MON$$      MODE GO,TEST
   MON$$      EXEQ FORTRAN,,,8,4,,,EIGN
    DIMENSION IPIVOT(38),INDEX(38,2)
    DIMENSION A(38,38),D(38),DUMMY(38)
  1 FORMAT(2F10.7)
  4 FORMAT(4F18.5)
 55 FORMAT(E16.6)
 99 FORMAT(I3)
333 FORMAT(13H  EIGENVALUES)
337 FORMAT(15H   EIGENVECTORS)
702 FORMAT(I3,I3)
802 FORMAT(6E13.6)
811 READ(1,702) (NRR,K )
    READ(1,1) (E1,E2)
    LL=NRR-K
    IF (LL)888,738,737
737 READ(1,802)(( A(I,J),J=1,LL),I=1,K)
    REWIND 5
    DO 719 I=1,K
    WRITE(5)(A(I,J),J=1,LL)
719 CONTINUE
    READ(1,802)(( A(I,J),J=1,LL),I=1,LL)
    N=LL
    DO 720 J=1,N
720 IPIVOT(J)=0
    DO 550 I=1,N
    AMAX=0.0
    DO 805 J=1,N
    IF(IPIVOT(J)-1)760,805,760
760 DO 800 KKK=1,N
    IF(IPIVOT(KKK)-1)779,800,740
779 LLLL=1
780 IF(ABS (AMAX)-ABS ( A(J,KKK)))785,800,800.
785 IROW=J
    ICOLUM=KKK
    AMAX= A(J,KKK)
800 CONTINUE
805 CONTINUE
    IPIVOT(ICOLUM)=IPIVOT(ICOLUM)+1
    IF(IROW-ICOLUM)140,260,140
140 DO 200 L=1,N
    SWAP= A(IROW,L)
     A(IROW,L)= A(ICOLUM,L)
200  A(ICOLUM,L)=SWAP
260 INDEX(I,1)=IROW
```

```
      INDEX(I,2)=ICOLUM
      DUMMY(I)= A(ICOLUM,ICOLUM)
       A(ICOLUM,ICOLUM)=1.0
      DO 350 L=1,N
350    A(ICOLUM,L)= A(ICOLUM,L)/DUMMY(I)
      DO 550 L1=1,N
      IF(L1-ICOLUM)400,550,400
400   T= A(L1,ICOLUM)
       A(L1,ICOLUM)=0.0
      DO 450 L=1,N
450    A(L1,L)= A(L1,L)- A(ICOLUM,L)*T
550   CONTINUE
      DO 710 I=1,N
      L=N+1-I
      IF(INDEX(L,1)-INDEX(L,2))630,710,630
630   JROW=INDEX(L,1)
      JCOLUM=INDEX(L,2)
      DO 705 KKK=1,N
      SWAP= A(KKK,JROW)
       A(KKK,JROW)= A(KKK,JCOLUM)
       A(KKK,JCOLUM)=SWAP
705   CONTINUE
710   CONTINUE
740   JDUM=1
      REWIND 4
      M3=LL
      REWIND 5
500   DO 501 I=1,K
      READ(5)(D(IMJ),IMJ=1,LL)
      DO 502 J=1,M3
      SUM=0.0
      DO 503 JJ=1,LL
      SUM =SUM+D(JJ)*A(JJ,J)
503   CONTINUE
      DUMMY(J)=SUM
502   CONTINUE
      WRITE(4)(DUMMY(IMJ),IMJ=1,M3)
501   CONTINUE
      JDUM=JDUM-1
      REWIND  4
      IF(JDUM)506,504,888
504   REWIND 5
      REWIND 4
      DO 505 J=1,K
      READ(4)(DUMMY(I),I=1,M3)
      WRITE(5)(DUMMY(I),I=1,M3)
505   CONTINUE
      REWIND 4
      REWIND 5
      M3=K
```

```
      GO TO 500
  506 READ(1,802)(DUMMY(I),I=1,K)
  738 DO 998 I=1,K
      READ(1,802)(A(I,J),J=1,K)
  998 CONTINUE
      IF(LL)688,741,742
  742 DO 712 I=1,K
      READ(4)(D(IMJ),IMJ=1,K)
      DO 712 J=1,K
      A(I,J)=A(I,J)-D(J)
      A(I,J)=A(I,J)*DUMMY(I)*DUMMY(J)
  712 CONTINUE
  741 N=K
      M=N-1
      IJKK=0
      REWIND 5
   20 II=1
      JJ=2
      I=1
      J=1
   98 J=J+1
      IF(ABS (A(I,J))-E1)103,109,109
  103 IF(J-N)98,104,104
  104 IF(I-M)105,110,110
  105 I=I+1
      J=I
      GO TO 98
  110 IF(E1-E2)40,40,111
  111 E1=E1* .5
      GO TO 20
  109 II=I
      JJ=J
      GO TO 106
  106 IF(A(II,II)-A(JJ,JJ)) 12,13,12
   12 GAM=A(II,JJ)/(2.*(A(II,II)-A(JJ,JJ)))
      IF(ABS (GAM)-.4142)71,72,72
   71 S= 2. *GAM/(1.+GAM*GAM)
      C= (1.-GAM*GAM)/(1.+GAM*GAM)
      GO TO 14
   72 IF(GAM-.4142)73,13,13
   73 S=-.70710678
      C= .70710678
      GO TO 14
   13 C=.70710678
      S=.70710678
   14 DO 57 I=1,N
      BB=C*A(II,I)+S*A(JJ,I)
      A(JJ,I)=-S*A(II,I)+C*A(JJ,I)
      A(II,I)=BB
   57 CONTINUE
```

```
 61 DO 58 I=1,N
    BB=C*A(I,II)+S*A(I,JJ)
    A(I,JJ)=-S*A(I,II)+C*A(I,JJ)
    A(I,II)=BB
 58 CONTINUE
    IJKK=IJKK+1
    WRITE(5) IJKK,II,JJ,C,S
    I=II
    J=JJ
    GO TO 103
 40 WRITE(2,333)
    WRITE(2,55)(A(I,I),I=1,K)
997 DO 301 I=1,N
    DO 302 J=1,N
    A(I,J)=0.0
302 CONTINUE
    A(I,I)=1.0
301 CONTINUE
    M=IJKK
886 REWIND 5
885 READ(5)IJKK,II,JJ,C,S
    DO 303 I=1,N
    BB=C*A(I,II)+S*A(I,JJ)
    A(I,JJ)=-S*A(I,II)+C*A(I,JJ)
    A(I,II)=BB
303 CONTINUE
    IF(M-IJKK)888,887,885
887 WRITE(2,337)
    DO 307 J=1,N
    BB=A(1,J)
    DO 308 I=1,N
    A(I,J)=A(I,J)/BB
308 CONTINUE
    WRITE (2,99)  J
    WRITE(2,4)(A(I,J),I=1,N )
307 CONTINUE
    GO TO 811
888 STOP
    END
   MON$$      EXEQ LINKLOAD
              CALL EIGN
   MON$$      EXEQ EIGN,MJB
```

EXAMPLE DATA FOR PROGRAM 1

U = .25 EQL = 1.0 NRR = 25 K = 10 NT = 32

```
.25  1.0   25 10 32
 1 1.0    .125
 2 1.0    .875
 3 1.0    .125
 4 1.0   1.0
 5 1.0    .875
 6 1.0    .125
 7 1.0   1.0
 8 1.0   1.0
 9 1.0    .875
10 1.025  .125
11
12
13
14
15
16
17
18
19
20
21
22          .375
23          .50
24          .50
25          .50
26          .50
27 0.0   0.0
28 1.75   .125
29 2.0    .875
30 2.0   1.0
31 2.0   1.0
32 2.0   1.0
```

```
14 15  3  2 30  4 11 28 12 13    29
 3 16  5  4 31  7 12 29  1 14  0 30
16 17  6  5  4  8 13  1 14 15 30  2
 5  6  8  7 32 25  1 30  2  3  0 31
 6 18  9  8  7 24 14  2  3 16 31  4
18 19 10  9  8 23 15  3 16 17  4  5
 8  9 24 25 26  0  2 31  4  5  0 32
 9 10 23 24 25  0  3  4  5  6 32  7
10 20 22 23 24  0 16  5  6 18  7  8
20  0 21 22 23  0 17  6 18 19  8  9
 0  0 13 12 28  1  0  0  0  0  0 27
13  0 14  1 29  2  0 27 11 00  0 28
 0  0 15 14  1  3  0 11  0  0 28 12
15  0 16  3  2  5  0 12 13  0 29  1
 0  0 17 16  3  6  0 13  0  0  1 14
17  0 18  6  5  9  0 14 15  0  2  3
 0  0 19 18  6 10  0 15  0  0  3 16
19  0 20 10  9 22  0 16 17  0  5  6
 0  0  - 20 10 21  0 17  0  0  6 18
 0  0    21 22  0  0 18 19  0  9 10
 0                   19 10 20  0 23 22
21  0  0  0  0  0 18  9 10 20 24 23
22 21  0  0  0  0  6  8  9 10 25 24
23 22  0  0  0  0  5  7  8  9 26 25
24 23  0  0  0  0  4 32  7  8  0 26
25 24  0  0  0  0 31  0 32  7  0  0
```

EXAMPLE OUTPUT FROM PROGRAM 2

EIGENVALUES

.314837E 02
.865329E 02
.627289E 02
.515693E 02
.114069E 02
.284834E 02
.184671E 02
.410978E 02
.395978E 01
.209339E 02

EIGENVECTORS

1					
	1.000	.504	3.919	-4.702	-.293
	-2.720	-1.458	3.838	.328	-4.791
2					
	1.000	-2.267	2.144	2.594	-2.472
	1.389	-1.203	1.881	-.935	.349
3					
	1.000	-1.415	.516	.539	.784
	-.937	.122	-1.206	.945	-.501
4					
	1.000	-.805	1.902	-2.127	-.257
	1.812	3.692	-.682	-.884	1.023
5					
	1.000	2.814	1.612	2.353	.777
	-1.008	.852	-1.167	-3.037	-1.364
6					
	1.000	.189	-.951	.064	-.340
	1.054	.159	-.066	.256	-1.275
7					
	1.000	1.276	1.219	-.516	.310
	1.193	-1.710	-.967	.904	.958
8					
	1.000	-.302	-.546	-.294	.777
	-.160	-.331	.567	-.782	.564
9					
	1.000	-3.817	-3.626	-7.821	-12.734
	-4.998	-6.692	-12.323	-9.772	-.368
10					
	1.000	.748	-.249	.176	-1.088
	-1.032	.605	.383	.781	.740

NATURAL FREQUENCIES OF CANTILEVERED TRIANGULAR TAPERED PLATES

by

DALLAS R. KOERNER

B. S., Kansas State University, 1963

AN ABSTRACT OF A MASTER'S THESIS

submitted in partial fulfillment of the

requirements for the degree

MASTER OF SCIENCE

Department of Civil Engineering

KANSAS STATE UNIVERSITY

1966

The natural frequencies and mode shapes for a series of cantilevered triangular tapered plates were computed by a method first introduced by John Houbolt in his doctoral thesis. This method of analysis utilizes finite-difference equations in conjunction with the principle of minimum potential energy. To be used to its full potential Houbolt's method of analysis requires the use of high-speed computing equipment.

Applications were made to cantilevered triangular tapered plates having four different planforms. Five different taper ratios were investigated for each planform.

Computed results are compared with results from previous investigations whenever possible. The computed results compare very well with those found in previous investigations.

It was found that the taper ratio has little effect on the magnitude of the first five natural frequencies if it does not exceed 0.6. The same is true for the nodal patterns. A definite change occurs only when the outer end of the plate gets relatively thin, as compared to the thickness at the fixed edge.